The Journal of Chemical Physics

Liquid structure of 1-alkyl-3-methylimidazolium-hexafluorophosphates by wide angle x-ray and neutron scattering and molecular dynamics

Cite as: J. Chem. Phys. **134**, 114521 (2011); https://doi.org/10.1063/1.3565458
Submitted: 09 November 2010 • Accepted: 23 February 2011 • Published Online: 18 March 2011

Marina Macchiagodena, Lorenzo Gontrani, Fabio Ramondo, et al.

View Online Export Citation

ARTICLES YOU MAY BE INTERESTED IN

Small angle neutron scattering from 1-alkyl-3-methylimidazolium hexafluorophosphate ionic liquids ($[C_n mim][PF_6]$, $n = 4$, 6, and 8)
The Journal of Chemical Physics **133**, 074510 (2010); https://doi.org/10.1063/1.3473825

Communication: X-ray scattering from ionic liquids with pyrrolidinium cations
The Journal of Chemical Physics **134**, 121101 (2011); https://doi.org/10.1063/1.3569131

TRAVIS—A free analyzer for trajectories from molecular simulation
The Journal of Chemical Physics **152**, 164105 (2020); https://doi.org/10.1063/5.0005078

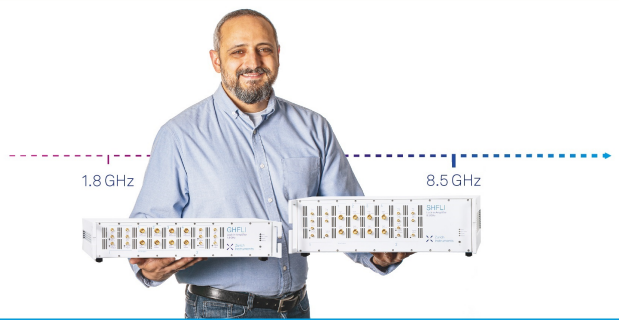

© 2011 American Institute of Physics.

AIP Publishing

Liquid structure of 1-alkyl-3-methylimidazolium-hexafluorophosphates by wide angle x-ray and neutron scattering and molecular dynamics

Marina Macchiagodena,[1] Lorenzo Gontrani,[2] Fabio Ramondo,[1,a)]
Alessandro Triolo,[3] and Ruggero Caminiti[2]
[1]*Department of Chemistry, Chemical Engineering and Materials, University of L'Aquila, via Vetoio, Coppito, I 67100 L'Aquila, Italy*
[2]*Department of Chemistry, University of Rome 'Sapienza', P.le Aldo Moro 5, I 00185 Rome, Italy*
[3]*CNR-Istituto di Struttura della Materia, Area della Ricerca di Roma 2, Tor Vergata, Rome, Italy*

(Received 9 November 2010; accepted 23 February 2011; published online 18 March 2011)

We report for the first time joined energy dispersed x-ray and neutron diffraction experiments on a series of (both protiated and selectively deuteriated) 1-alkyl-3-methylimidazolium hexafluorophosphate salts (alkyl = butyl, hexyl, octyl) at ambient conditions. The x-ray experimental data are used to optimize the interaction potential used for running molecular dynamics simulations on these systems. Such a potential leads to a good description of neutron scattering data from the samples without additional refinement, thus further validating the potential definition. The molecular dynamics simulations were used to access microscopic information on the morphology of the proposed systems, thus probing the role played by alkyl chain length on the structure. The comparison of x-ray weighted and neutron-weighted computed diffraction patterns allows the rationalization of several diffraction features. Further insight into cation–anion coordination and alkyl chain conformational equilibrium is provided on the basis of the MD-derived snapshots, confirming and extending previously obtained results on these issues. © *2011 American Institute of Physics*. [doi:10.1063/1.3565458]

I. INTRODUCTION

Ionic liquids are presently a hot research topic.[1–8] This large interest is the consequence of their several appealing properties, including low vapor pressure, nonflammability, chemical and thermal stability, high solvent capacity and conductivity, to mention a few of them. They are liquid composed solely of ionic species and their range of applications spans from electrochemistry,[9] to synthetic[10] and catalytic chemistry.[11] There is currently a trend to appropriately design ionic liquids according to the peculiar application they must serve for, by slight modulating their chemical architecture. The number of available cation–anion combinations has significantly increased and it is now possible, by changing the anion nature or varying the alkyl chain length in the cation, to achieve improved properties.

Since the structural properties are fundamental to explain and rationalize the physical and chemical properties of these materials, their structure determination is a topic of great interest, although hardly straightforward. The ionic liquids complexity stems from the various and sometimes competitive intermolecular interactions. The use of a combined approach, both theoretical and experimental, is therefore required in order to appropriately describe their structural and dynamical aspects. The role of computer simulations is important for various aspects[12–14] and accurate predictions are very often obtained from a combination of several theoretical approaches. Ionic liquids have been modeled in different states of aggregation, from crystals to liquids and clusters, and the competition between electrostatic, dispersion, and hydrogen-bonding interactions has been identified at the origin of observed structural patterns.[15] The long-range cation–anion Coulombic interactions are largely dominant for the isolated gas-phase ion pairs and detailed investigations on the magnitude and directionality of the interaction energies have been carried out on several ion couples by *ab initio* methods.[16–19] Interest in the ion pairs has also grown because the formation of neutral species in gas phase was one of the mechanisms of vaporization of ionic liquids.[20] Although the electrostatic interaction is the major force of attraction, close contacts between CH and the anion were found in the *ab initio* geometries of ion pairs[16–19] as well as in the structure of liquids[21] and crystals[22] of alkylimidazolium cations containing fluoroanions. Such evidences suggested the existence of local C–H···F interactions in some liquids which could give directional properties to the anion–cation interaction and explain several and alternative anion–cation local structures.[23] However, regarding the possibility to classify such interactions as hydrogen bonding, the question remains open[24] and *ab initio* studies[25,26] revealed that the nature of the CH···F interaction is different from that of conventional hydrogen bonds and this contact is not essential for the cation–anion attraction. As for gas phase, electrostatic interactions are significant also in the liquid state; however, by increasing the length of the alkyl chain, the short-range van der Waals interactions increase their role and become competitive with the electrostatic term. Heats of vaporization obtained from a series of ionic liquids[27] confirm that when van der Waals contribution enhances, the Coulomb forces are almost invariable. Consistently, x-ray diffraction

a)Electronic mail: fabio.ramondo@univaq.it.

 © 2011 American Institute of Physics

studies revealed that ionic liquids form heterogeneous "nanostructures" regions, the size of which is proportional to the alkyl chain length of the cation.[28–34] Further evidences of such segregation were found by the fact that the very long-chain 1-alkyl-3-methylimidazolium BF_4^- are low-melting mesomorphic crystalline solids at room temperature whereas the short chain analogs (n = 2–10) are isotropic ionic liquids.[35]

On one hand *ab initio* calculations allow accurate predictions on the local structures of ion pairs or anion–cation clusters of moderate size; on the other hand, molecular dynamics (MD) simulations provide a microscopic picture of the structure of the ionic liquids and offer the capability to predict several dynamic properties of the liquids, on the basis of classical interactions. Several progresses have been made in the application of MD simulations to ionic liquids since the first study performed in 2001 (Ref. 36) and now several levels of theory can be applied to simulate ionic liquids, from classical models to quantum chemical levels. Various thermodynamic properties of pure ionic liquids such as density, isothermal compressibility coefficient, cohesive energy density, the heat of vaporization, diffusive coefficients were compared with the experimental results and the theoretical models were developed to reproduce with accuracy of the experiments. Many of the force fields used for ionic liquid simulations, including AMBER,[37] CHARMM,[38] and OPLS,[39,40] were validated mainly on the basis of these thermodynamic properties: ionic liquid microscopic structures were eventually obtained assuming the validity of the various force fields. However, x-ray (as well as neutron) diffraction (one of the main source of experimental information on the liquids' structure), should be considered an important test for validating a force field, especially when the latter is to be used to describe structural details. A coarse grain model was constructed some years ago to calculate neutron and x-ray scattering structure functions of some 1-*n*-alkyl-3-methylimidazolium-hexafluorophosphates by molecular dynamics.[41] Simulations revealed intermediate range order in these liquids; however, the lack of wide angle x-ray scattering experimental data did not allow a comparison with the theoretical spectra.

The main aim of the present work is to report the results of an energy dispersive x-ray diffraction (EDXD) and neutron diffraction study on these ionic liquids by proposing, for the first time, a comparative investigation of such liquids through two experimental diffraction techniques and a theoretical description by molecular dynamics. In this work we focus our attention on one of the most studied classes of ionic liquid, 1-alkyl-3-methylimidazolium-hexafluorophosphates, $[C_n\text{mim}][PF_6]$, where $n-1$ indicates the number of CH_2 units in the side alkyl chain. The structure of the first member of the series $[C_1\text{mim}][PF_6]$ has been determined by x-ray diffraction in the crystal phase[42] and by neutron diffraction in the liquid phase.[43] Also the crystal structure of $[C_4\text{mim}][PF_6]$ has been the subject of x-ray investigations[44,45] whereas the structure of liquid $[C_4\text{mim}][PF_6]$ has been studied by x-ray[46] as well as neutron[47] diffraction experiments. Recently Hardacre *et al.* reported on small angle neutron scattering data from a series of selectively deuteriated $[C_n\text{mim}][PF_6]$, with n = 4, 6, 8, paying special attention to the low q portion of the datasets.[48]

The combined approach here proposed is applied to the following ionic liquids: 1-alkyl-3-methylimidazolium-hexafluorophosphates (alkyl = *n*-butyl ($[C_4\text{mim}][PF_6]$ also indicated as [bmim] $[PF_6]$), hexyl ($[C_6\text{mim}][PF_6]$ also indicated as [hmim] $[PF_6]$), and octyl ($[C_8\text{mim}]$ also indicated as $[\text{omim}][PF_6]$)). The comparison between cations with short alkyl chain and cations with relatively long alkyl chain allows to investigate how properties and structure of ionic liquids may change as a function of the alkyl chain length. MD simulations were carried out (on the basis of a modified OPLS force field[40]) and the results have been compared with those of x-ray and neutron diffraction experiments. As proposed in previous studies,[49–63] comparing the experimental and theoretical structure functions provide both a tool to validate our computational protocol and for detailed interpretation of experimental data. For example, the lack of agreement with experimental diffraction data could reveal inadequacy of some parameters of the force field in describing some intermolecular interactions.[53] The proposed comparison between x-ray, neutron diffraction, and MD simulations validates our theoretical models and allows describing some important structural aspects such as the cation–anion distribution in the liquid, the orientation of the alkyl-chain with respect to the imidazolium ring, and the conformation of the alkyl-chain. It is worth observing that conformational isomerism of 1-alkyl-3-methylimidazolium cations is fundamental in liquid solid phase transition processes.[64,65]

II. EXPERIMENTAL DETAILS

A. X-ray diffraction

The large angle x-ray scattering experiments were performed using the noncommercial energy-scanning diffractometer built in the Department of Chemistry at the University "La Sapienza" of Rome (Patent no. 01126484—June 23, 1993). Detailed description of instrument, technique, and the experimental protocol (instrument geometry and scattering angles) of the data acquisition phase can be found elsewhere.[49–56] The appropriate measuring time (i.e., number of counts) was chosen to obtain scattering variable (q) spectra with high signal to noise ratio (600 000 counts on average).

The expression of q is

$$q = \frac{4\pi \sin\vartheta}{\lambda} = E\,1.014\,\sin\vartheta,$$

where E is expressed in keV and q in Å^{-1}. The various angular data were processed according to the procedure described in literature,[49–56] normalized to a stoichiometric unit of volume containing one ionic couple and combined to yield the total "(static) structure function," $I(q)$, which is equal to

$$I(q) = I_{\text{e.u.}} - \sum_{i=1}^{n} x_i f_i^2$$

where f_i are the atomic scattering factors, x_i are the number concentrations of the i-type atoms in the stoichiometric unit

(i.e., the group of particles used as reference for data normalization, the ion pair in this case), and $I_{\text{e.u.}}$ is the observed intensity in electron units (electrons^2). Fourier transform of $I(q)$ led to radial distribution function (RDF)

$$D(r) = 4\pi r^2\rho_0 + \frac{2r}{\pi}\int_0^{q_{\max}} qI(q)M(q)\,\sin(rq)dq.$$

In the equation, ρ_0 (electrons^2/Å^3) is the bulk number density of stoichiometer units and

$$M(q) = \frac{f_N^2(0)}{f_N^2(q)}e^{-0.01q^2}$$

is the modification factor. In experimental results we report the Diff(r) function instead of $D(r)$ function, so defined as

$$\text{Diff}(r) = D(r) - 4\pi r^2\rho_0.$$

B. Neutron diffraction

Neutron diffraction measurements were performed on the three protiated liquids and on a series of selectively deuteriated samples. Along with the parent compounds, two samples were obtained by selective deuterations of the methyl group and the alkyl group whereas a third sample was derived from the complete deuteration[48] following the procedure described in Ref. 66.

Neutron scattering data were collected using SANDALS at the ISIS pulsed neutron and muon source at the Rutherford Appleton Laboratory, UK. The instrument has a wavelength range of 0.05–4.5 Å, and data were collected over the q range 0.05–50 Å^{-1}. Each sample was contained in "null scattering" $Ti_{0.68}Zr_{0.32}$ flat plate cells of internal geometry of 1 mm × 35 mm × 35 mm with a wall thickness of 1 mm. During measurements, the cell was maintained at a temperature of 323 K using a Julabo circulating heater. Measurements were made on each of the empty sample holders, the empty spectrometer, and a 3.1 mm thick vanadium standard sample for the purposes of instrument calibration and data normalization. After appropriate normalization for the cell and the window material, good reproducibility was found between the sample cells.

Data analysis was performed using GUDRUN, based upon algorithms in the ATLAS package,[67,68] to produce a differential scattering cross section for each sample. The experimental sample densities and scattering levels were consistent with the correct isotopic compositions of the samples. Calibration and background subtraction for single atom scattering[69] were made to produce a differential scattering cross section for each sample.

III. COMPUTATIONAL DETAILS

The force field OPLS-All Atoms (OPLS-AA), developed by Canongia Lopes and Pádua,[40] was our reference for the molecular models. This force field reproduces, with good accuracy, some important properties of most ionic liquids such as densities and vaporization enthalpies. However, focusing our attention mainly on the structure of ionic liquids, the molecular models adopted should be sufficiently accurate to describe both bulk properties and the experimental diffraction data. In order to select a reliable force field, we tested the original OPLS-AA (Ref. 40) potential to reproduce both density and experimental x-ray diffraction data. The best match was obtained refining the starting force field by adopting the partial atomic charges and the torsional Fourier coefficients suggested by a recent study[70] for [1-alkyl-3-methylimidazolium][PF_6]. Concerning the intramolecular bond distances of the cation and anion, we inserted in the force field some restraints assuming the values observed in the [mmim][PF_6] crystal.[43] Nonbonded interactions were computed up to 8 Å. As suggested from previous studies,[53] larger cutoff value sets should not affect the quality of the results largely.

The molecular dynamics simulations were performed using the DL_POLY package.[71,72] The cubic boxes consisted of 343 ionic pairs and periodic boundary conditions were

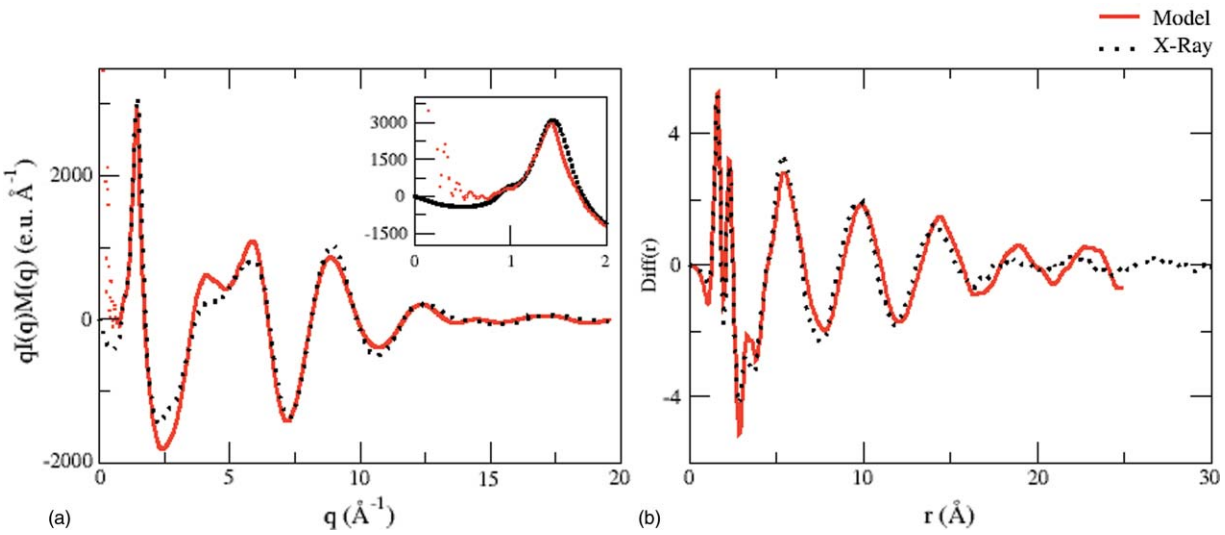

FIG. 1. Experimental and theoretical structure functions, $qI(q)M(q)$, (a) and Diff(r) (b) of [bmim][PF_6]. In the inset the low q portion is reported.

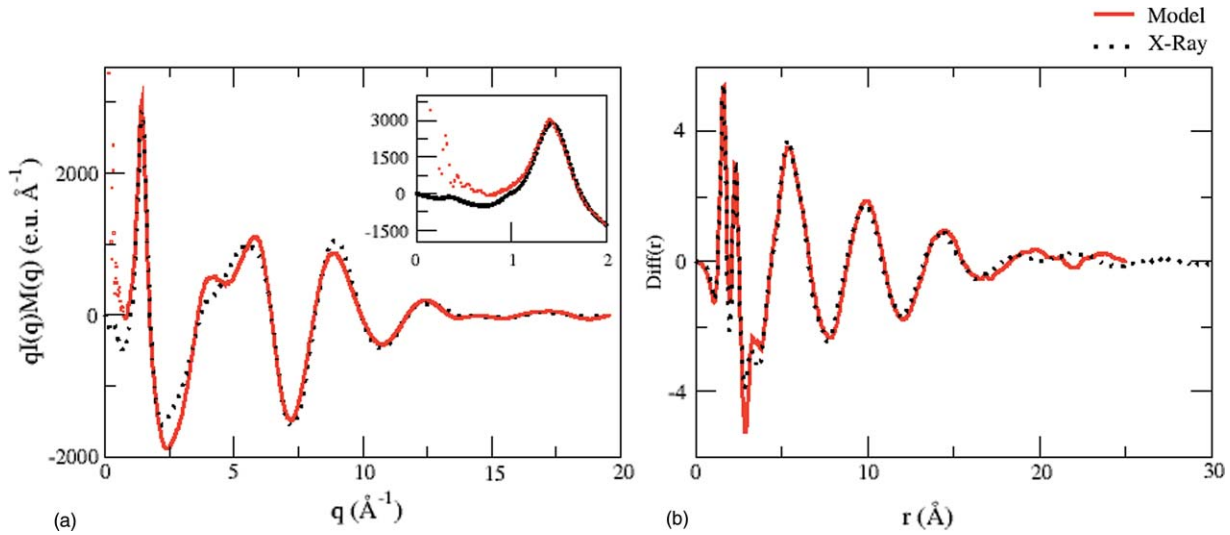

FIG. 2. Experimental and theoretical structure functions, $qI(q)M(q)$, (a) and Diff(r) (b) of [hmim][PF_6]. In the inset the low q portion is reported.

applied. The box dimensions were 49.06 Å for [bmim][PF_6], 51.54 Å for [hmim][PF_6], and 53.85 Å for [omim][PF_6]. After a short initial minimization, the volume of the system was lowered with some *NpT* simulations (10 000 steps of 1 fs each) using the Hoover–Nose thermostat at high pressure (order $\sim 10^3$ atm) and temperature of 300 K. The pressure of the system was then lowered at 1 atm followed by 1 ns simulations for *NpT* equilibration and by 10 ns with a time step = 2 fs, in the same Hoover *NpT* ensemble. The system was regarded as equilibrated, when the fluctuations in the density and in the temperature were less than 1%. MD simulations were then performed for 5 ns with a time step = 2 fs, in the *NVT* ensemble.

In order to compare with the corresponding experimental quantities, the model x-ray/neutron scattering functions were obtained from the Debye function for all the $n \times (n-1)/2$ atomic pairs,[49–52] intra- as well as intermolecular pairs.

The expression for model $I(q)$ is

$$I(q)^{\mathrm{MODEL}} = \sum_{m>n} x_m x_m f_m(q) f_n(q) \frac{\sin(r_{mn} q)}{r_{mn} q}.$$

The indexes m and n refer to different atoms, x_m are the numerical concentrations in the "stoichiometric unit," $f_m(q)$ are the x-ray scattering factor or neutron coherent scattering length of the atomic/isotopic species, and r_{mn} is their distance; the configuration considered was the minimum image structure of the simulated periodic system. The function was then multiplied by q and by the same modification factor used for experimental data, thus obtaining a theoretical $qI(q)M(q)$ that is directly comparable to the experimental counterpart. Fourier transform of the $qI(q)M(q)$ led to the model radial distribution function. It is important to point out that in the very low q range ($q < 1$ Å^{-1}), the theoretical $I(q)$ is unreliable due to both the limited box size and the Debye formula we have used. We therefore cut our simulated

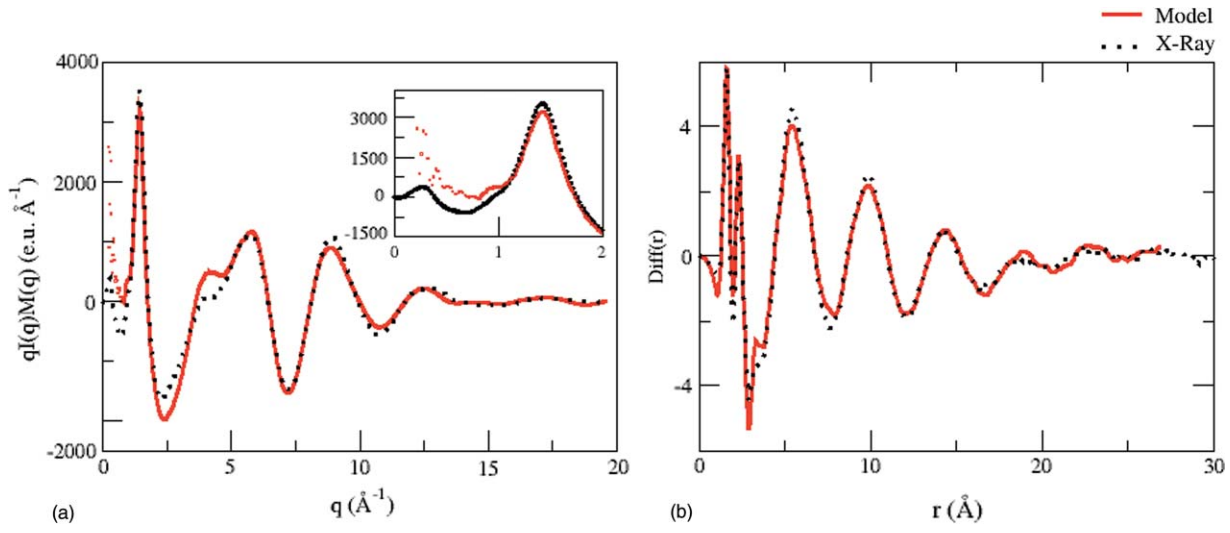

FIG. 3. Experimental and theoretical structure functions, $qI(q)M(q)$, (a) and Diff(r) (b) of [omim][PF_6]. In the inset the low q portion is reported.

values at $q \sim 0.8$ Å^{-1} and smoothly joined them with the experimental low q sets of data before performing the integration.

IV. RESULTS AND DISCUSSION

Since molecular dynamics is a powerful tool to investigate the properties of ionic liquids, a large number of MD simulations have been performed on 1-alkyl-3-methylimidazolium [PF_6] with particular attention to [bmim][PF_6]. Results from classical MD (Refs. 73–79) and Monte Carlo[80] simulations were reported using all-atom force fields[73–77] and united-atom models.[78,79] The pure liquid[81] and its mixture with CO_2 (Ref. 82) were also the subject of *ab initio* molecular dynamics (AIMD) studies through the Car–Parrinello method. Very recently MD simulations were carried out on [omim][PF_6] and [decyl-mim][PF_6] with boxes having adequate sizes to properly describe data at small q values.[83]

The present investigation adopts a modified version of the all-atom OPLS-type force field. The performance of our model was firstly tested against the liquid densities of each species. The results and the experimental densities are compared in Table I. As a matter of fact experimentally derived density values can be dramatically affected by trace amounts of impurities such as water[95] or other compounds[96] and this explains the wide spread of the value reported. Still the values obtained from our force field are in a general good agreement with the experimental data. In addition the present force field tends to better reproduce the density values than previous simulations.[70]

To further test the validity of the force field the enthalpy of vaporization was calculated. The molar enthalpy of vaporization at 1 atm pressure was calculated with the expression $\Delta_l^g H_m^0(T) = \Delta_l^g U_{c,m}^0(T) + RT$, where $\Delta_l^g U_{c,m}^0(T)$ is the *ensemble* average molar configurational energy obtained from the simulation.[27] The vapor phase was assumed to be formed by isolated molecules in the *NVT* ensemble and was simulated for an equal period of time. The values obtained at 300 K are 191.34 kJ mol^{-1} for [bmim][PF_6], 201.68 kJ mol^{-1} for [hmim][PF_6], and 208.39 kJ mol^{-1} for [omim][PF_6]. Unfortunately it is hard to evaluate the accuracy of these results on the basis of the spread experimental values given in literature, 154.8 kJ mol^{-1} (Ref. 97) and 189 kJ mol^{-1} (Ref. 98) for [bmim][PF_6], 139.8 kJ mol^{-1} for [hmim][PF_6] (Ref. 97), and 169(4) kJ mol^{-1} (Ref. 99) and 144.3 kJ mol^{-1} (Ref. 97) for [omim][PF_6]. However, the values obtained from our simulations show an increase of the cohesive energy with the length of the alkylic chain in line with that predicted for other series of ionic liquids.[27]

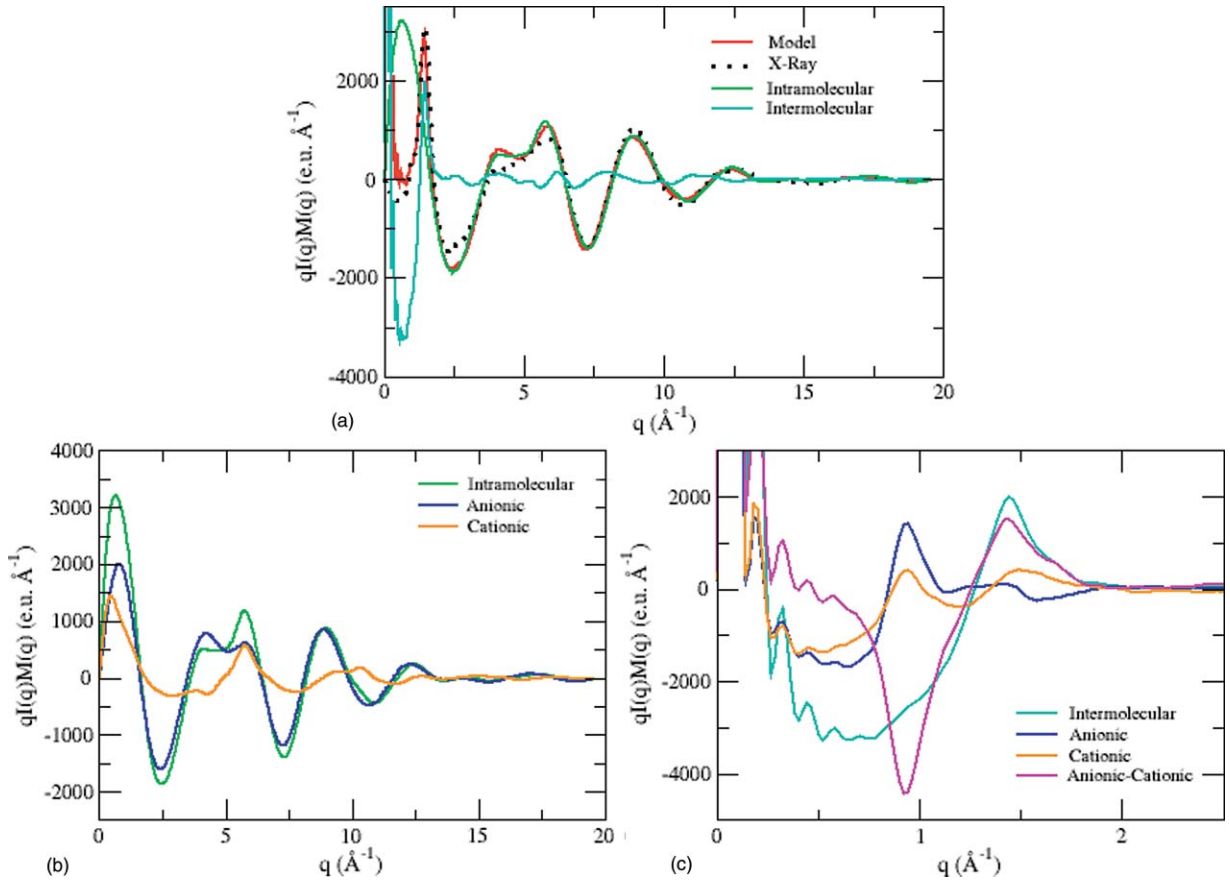

FIG. 4. Partial structure functions for [bmim][PF_6] obtained from MD simulations: (a) comparison between the total function and the intermolecular and intramolecular functions; (b) anionic and cationic contributions to the total intramolecular structure function; (c) anionic/anionic, cationic/cationic and cationic/anionic contributions to the total intermolecular structure function.

TABLE I. Simulated ρ_{MD} (g/cm^3) and experimental ρ_{exp} (g/cm^3) (T = 298 K) density of [1-alkyl-3-methylimidazolium][PF_6].

	ρ_{MD}	ρ_{exp}
[bmim][PF_6]	1.383(5)[a], 1.339[b]	1.3603[c]; 1.3564[c]; 1.368[d]; 1.371[e]; 1.362[f]; 1.37[g]; 1.367[h]; 1.3673[i]
[hmim][PF_6]	1.296(5)[a], 1.257[b]	1.29[g]; 1.292[d]; 1.29341[j]; 1.2935[k] ; 1.2937[l];1.278[m]
[omim][PF_6]	1.242(4)[a], 1.181[b]	1.22[g]; 1.23572[i]; 1.237[d]; 1.2245[c]; 1.2207[c]

[a]This work; uncertainty derived from NPT simulations are expressed as standard deviation in the last digit.
[b]Reference 70.
[c]Reference 84.
[d]Reference 85.
[e]Reference 86.
[f]Reference 87.
[g]Reference 88.
[h]Reference 89.
[i]Reference 90.
[j]Reference 91.
[k]Reference 92.
[l]Reference 93.
[m]Reference 94.

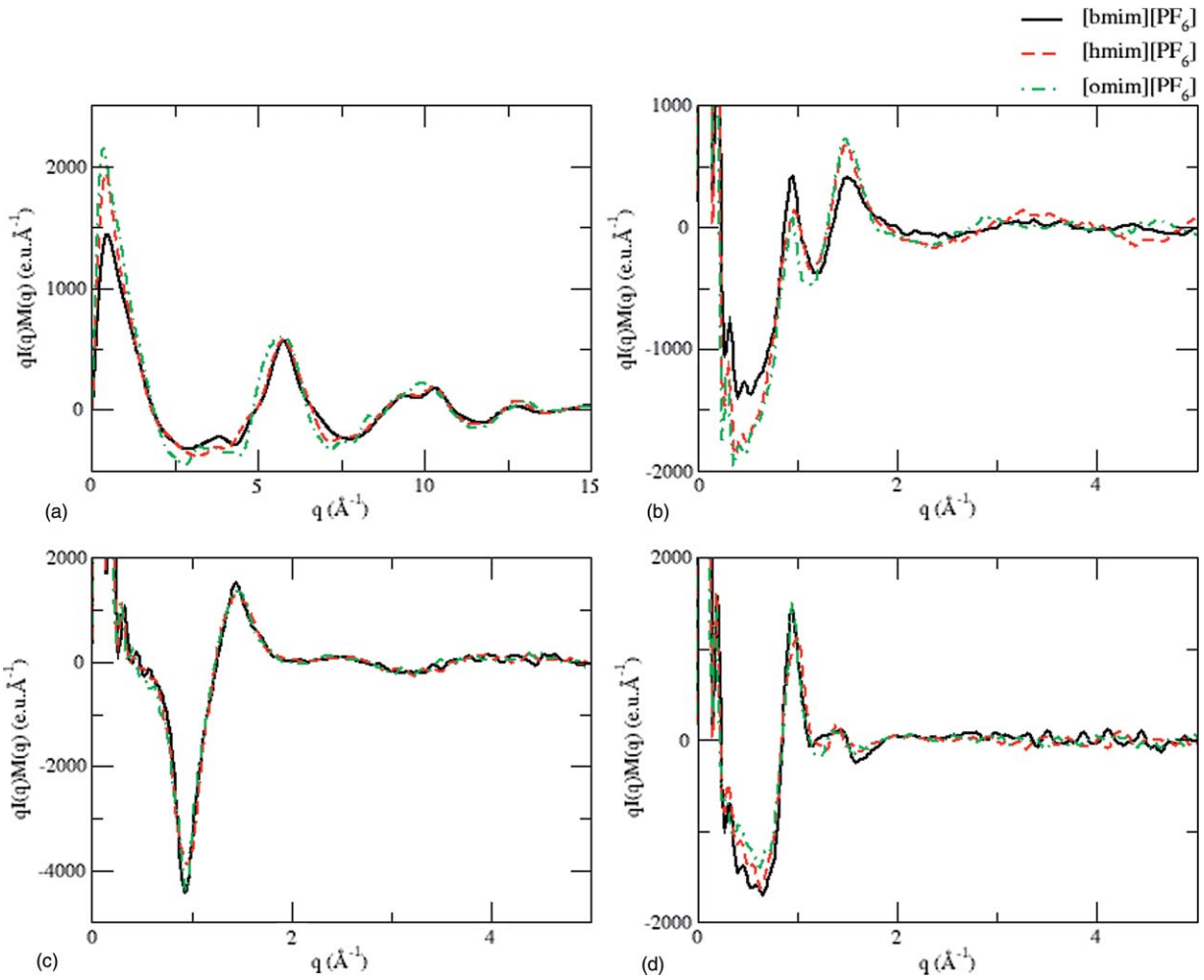

FIG. 5. Cationic intramolecular (a), cationic/cationic intermolecular (b), cationic/anionic intermolecular (c), and anionic intermolecular (d) partial structure functions for [bmim][PF_6], [hmim][PF_6], and [omim][PF_6] obtained from MD simulations.

V. STRUCTURAL ANALYSIS

A. Comparison with x-ray and neutron diffraction data

The structure function model $qI(q)M(q)$, derived from the last 5 ns molecular dynamics, is compared in Figs. 1(a), 2(a), and 3(a) with the corresponding experimental function. For each molecular species the radial distribution functions, Diff(r), are also reported [Figs. 1(b), 2(b) and 3(b)].

As seen, the experimental curve is well reproduced by simulations with agreement progressively improving in the series [bmim], [hmim], and [omim]. In particular, [bmim][PF_6] structure functions in Fig. 1(a) show good agreement for $q < 2$ Å^{-1} and $q > 6$ Å^{-1} whereas the peaks in the central region, 2–6 Å^{-1}, are reproduced with lower accuracy. On the other hand, the agreement is much better in a larger q range for [hmim][PF_6] [Fig. 2(a)] and [omim][PF_6] [Fig. 3(a)]. The origin of the discrepancy at intermediate q values between experimental and theoretical data of [bmim][PF6] could probably be due to the nonbonded terms involving the anion and the partially charged carbons of the ring. However, our attempts to modify partial charges in the specific force fields have not led to an improvement of the agreement. Another possibility might be the presence of specific interactions CH···F between the acidic H of the ring and F, expected more important for the smaller [bmim][PF_6] system. This possibility is not accounted for in the current implementation of the field and is worth investigating.

$I(q)$ for [bmim][PF_6] has been previously measured by using a $\theta-\theta$ x-ray diffractometer.[46] Notwithstanding the comparison with our data is not immediate since the authors do not adopt any modification factor, the main peaks are present in both the experiments. As well known, features at $q > 2$ Å^{-1} are expected largely due to intramolecular contributions. The analysis of intra- and intermolecular contributions to the experimental $I(q)$ has been carried out in the previous x-ray study of liquid [bmim][PF_6].[46] The x-ray total distribution functions showed a first prominent peak at $r = 1.6$ Å, assigned to the P–F pairs in [PF_6], and a second peak at $r = 2.3$ Å, mainly attributable to the F–F pairs in [PF_6] and to the correlations between the second-nearest atoms in the imidazolium ring of [bmim]. Such features are mainly found in our curves for [bmim] as well as [hmim] and [omim]. The curves of the present investigation also show features typical of some imidazolium-based systems with moderately long alkyl chains and with spherical and highly symmetric anions. The presence of two peaks at about 0.5 and 1.5 Å^{-1} and a shoulder around 0.9 Å^{-1} is in agreement with the previous findings from some of us[34] and the recent results from

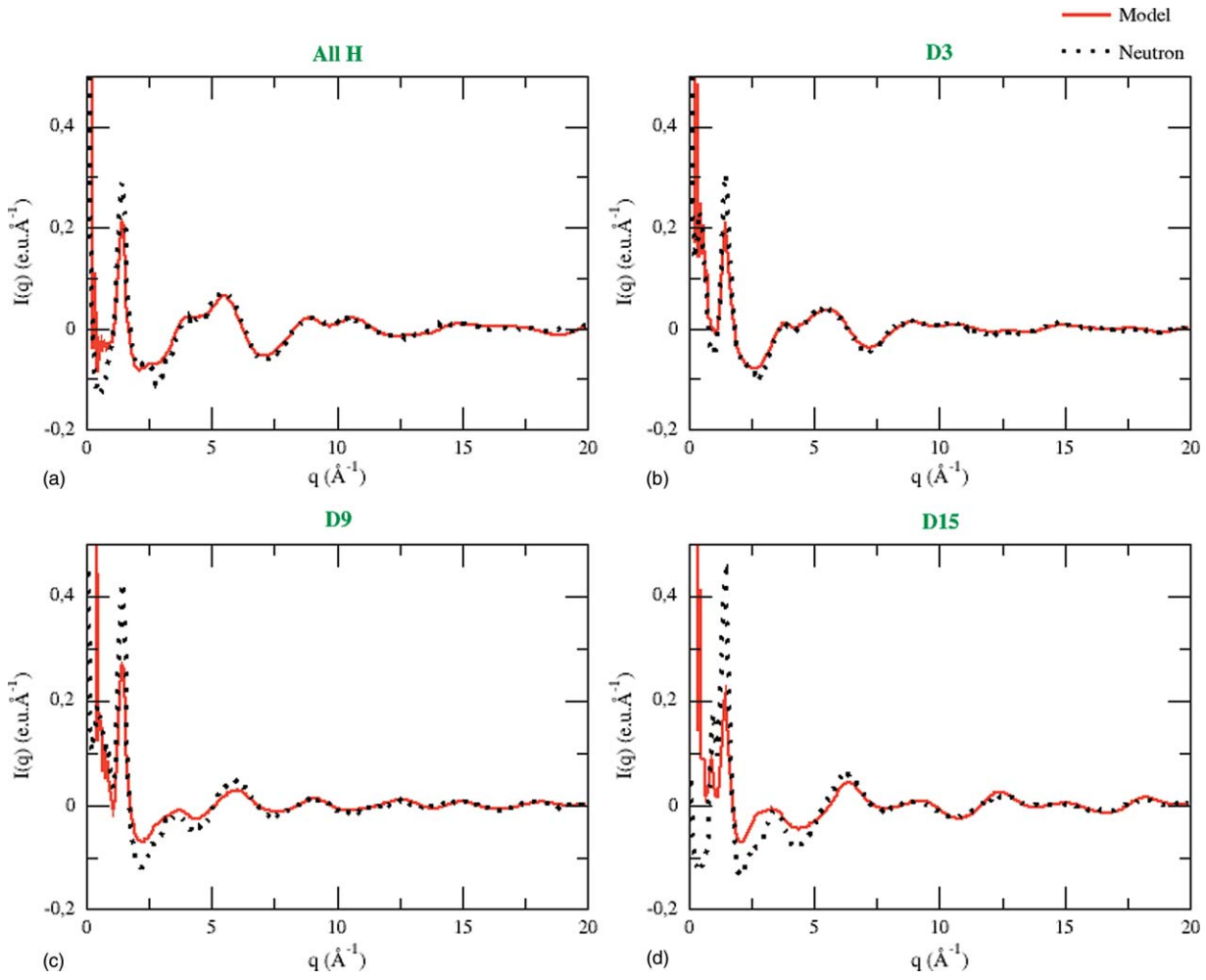

FIG. 6. Comparison between neutron structure functions obtained from experiment and MD simulations for [bmim] (a), 1-butyl-3-deuteriomethylimidazolium (b), 1-deuteriobuyl-3-methylimidazolium (c), and 1-deuteriobutyl-3-deuteriomethylimidazolium (d) [PF_6].

Hardacre *et al*.[48] Similarities are also present with the experimental curves of the system consisting of the smaller ethylmethylimidazolium cation and bromide anion.[59] Different interpretations have been instead proposed to explain the origin of the features at low q values. The recent study of Margulis *et al.*[83] combines structure functions calculated in detail for solids and liquids with evidences from experimental data. The peak at about 0.9 $Å^{-1}$ is observed both in the solid and in the liquid phase and is assigned to distances between strongly scattering polar groups separated from alkylic tails in agreement with the interpretation of Hardacre *et al*.[48] However, the existence of complex morphologies in ionic liquids cannot be excluded on the basis of the Margulis investigation.[83]

Notwithstanding, as we have pointed out above, the very low q region could be precluded to very accurate computations, it would be worth exploring anyway such region on the ground of our simulations data to estimate the role of the different contributions in the observed peaks, at least for $q > 0.8$ $Å^{-1}$. As a matter of fact further simulations were carried out by increasing the box dimension in order to estimate the quality of our simulations in reproducing the experimental data in large q ranges. However, the application to large boxes of the all-atom force field used for our simulation is yet a prohibitive task. Attempts were made enlarging twice the simulation box along one dimension, but the improvements obtained on the curve were indeed too small. Very recently Margulis *et al.*[83] analyzed with great attention the origin of first diffraction peaks using several computational techniques and adequate box sizes. Moreover, such an investigation[83] revealed a dependency on the intensity (not on the position) of the peaks simulated at low q values from the box size. We therefore analyze the pair partial structure functions for each molecular system from our models by isolating some significant contributions.

We discuss the results of the single contributions to the structure functions starting from [bmim][PF_6]. As a preliminary analysis, we factorized the total structure function into two contributions, an intramolecular term and an intermolecular one: the relative partial curves are shown in Fig. 4(a). In agreement with the previous x-ray investigation[46] intramolecular contributions account for the peaks at $q > 2$ $Å^{-1}$, whereas intermolecular ones contribute only at low q values.

Each partial structure function can be further factorized. Concerning the intramolecular function, we separated the cation contribution from anion one [Fig. 4(b)]. From such a decomposition, it is evident that the intramolecular structure function is largely dominated by the anion contribution in agreement with the assignment of Ref. 46.

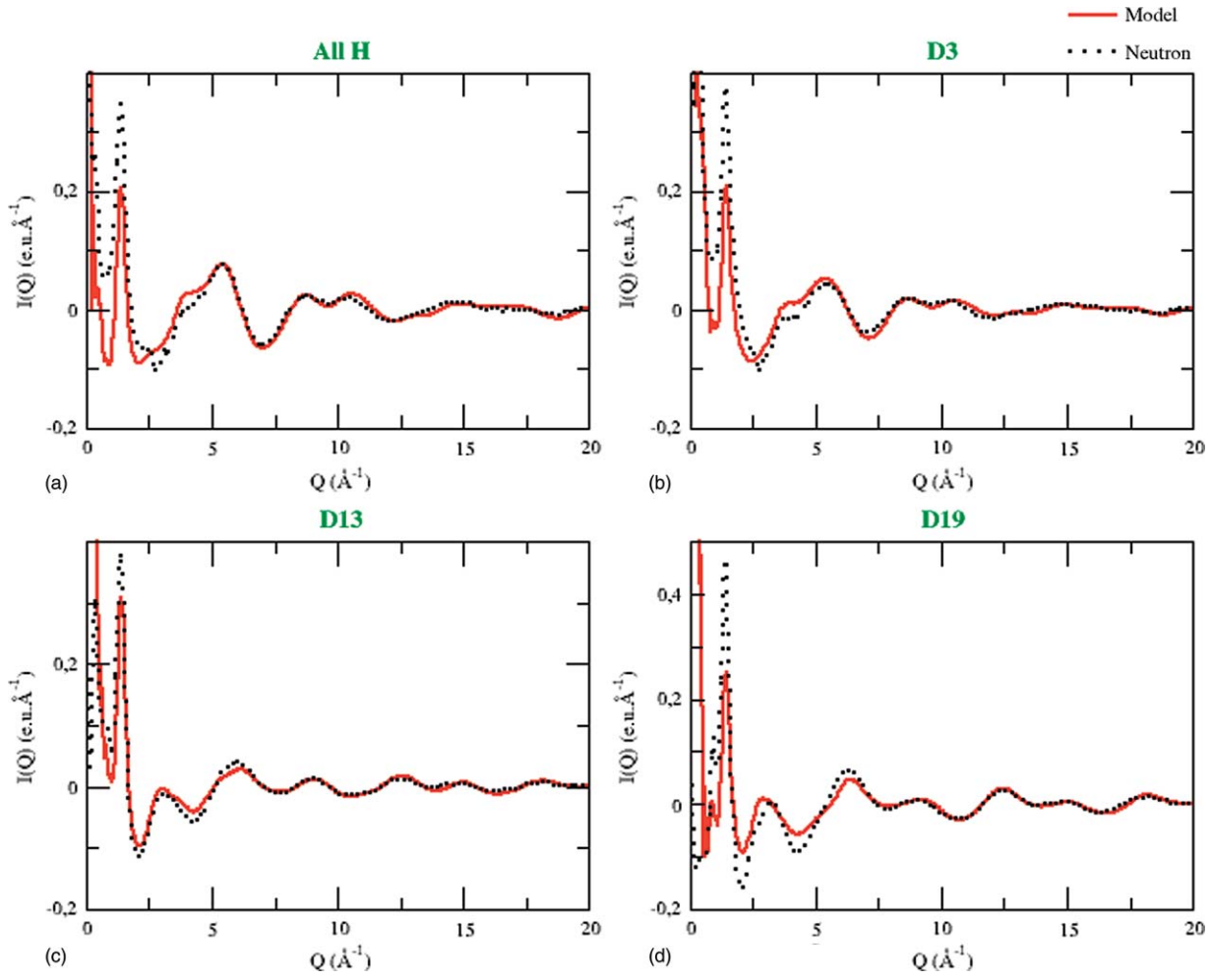

FIG. 7. Comparison between neutron structure functions obtained from experiment and MD simulations for [hmim] (a), 1-hexyl-3-deuteriomethylimidazolium (b), 1-deuteriohexyl-3-methylimidazolium (c), and 1-deuteriohexyl-3-deuteriomethylimidazolium (d) [PF_6].

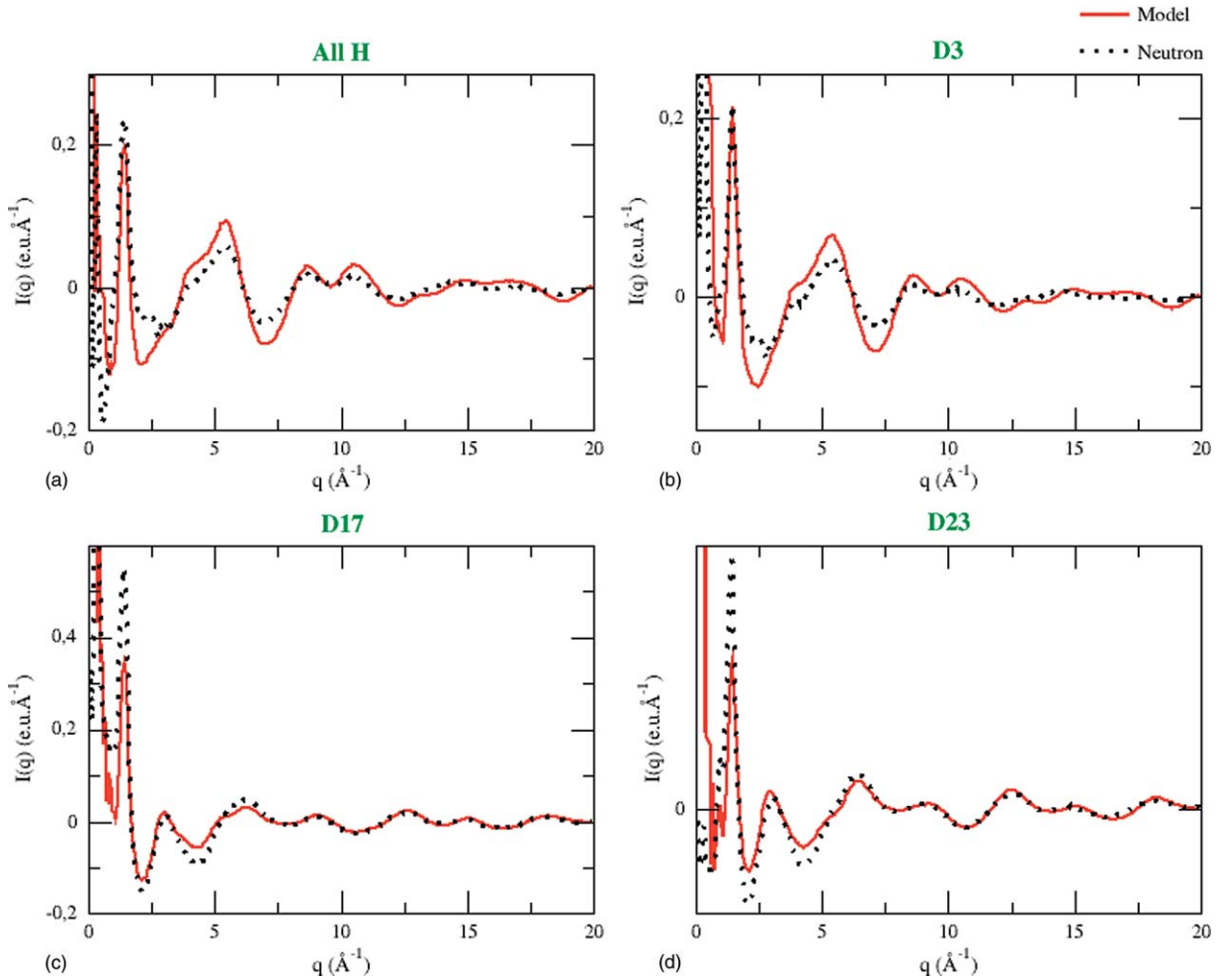

FIG. 8. Comparison between neutron structure functions obtained from experiment and MD simulations for [omim] (a), 1-octyl-3-deuteriomethylimidazolium (b), 1-deuteriooctyl-3-methylimidazolium (c), and 1-deuteriooctyl-3-deuteriomethylimidazolium (d) [PF_6].

Similarly, also for the case of the intermolecular function we distinguished the role of the cation–cation, anion–anion, and cation–anion pairs [Fig. 4(c)]. The cation–anion correlation plays a positive role at $q \approx 0.3$ Å^{-1} and $q \approx 1.48$ Å^{-1} whereas it contributes with negative values in the intermediate range (about 1 Å^{-1}). Both the cation–cation and anion–anion terms are instead contributing in the range around 0.95 Å^{-1}. This is consistent with the detailed dissection of $I(q)$ in atomic components proposed by Margulis *et al.*[83] In this region in fact the N···P and N···F components (cation–anion) were found with negative contributions of similar magnitude to the positive contributions of the cation–cation and anion–anion terms. Figure 4(c) reveals that all terms contribute to the lowest q peak whereas the cation–anion term is important to the peak centered at 1.48 Å^{-1}. Moreover, we stress that the cation–cation correlation contributes in a non-negligible way to such a peak. In conclusion, the superposition of the three partial functions leads to large contributions at $q \approx 0.3$ Å^{-1} and $q \approx 1.48$ Å^{-1} in agreement with the features observed at the same q values in the structure function reproduced in Fig. 4(c).

The analysis of the partial structure functions has been then applied to [hmim][PF_6] and [omim][PF_6] in order to investigate if the role of inter- and intramolecular interactions changes in the three systems (see Fig. 5) and to rationalize the experimental data reported in Figs. 1(a), 2(a) and 3(a). Concerning the intramolecular term, the anion contribution (data not shown) is essentially unaffected by the alkyl chain length. On the other hand, the cation contribution shows an appreciable dependence [Fig. 5(a)] mostly concerning the peaks at low q values, whose amplitude increases with the alkyl chain length.

Concerning the intermolecular term, the cation–cation contribution [Fig. 5(b)] shows a dependence from the alkyl chain length. Monitoring the amplitudes of the two peaks where this dependence is appreciable ($q \approx 0.95$ Å^{-1} and $q \approx 1.48$ Å^{-1}), we observe that the amplitude of the lower q one decreases whereas the amplitude of the second one increases with the alkyl chain length. On the other hand, the cation–anion term [Fig. 5(c)] shows no appreciable alkyl chain dependence. These evidences, together with the findings of Fig. 4(c), indicate that the experimentally observed dependence of peaks' amplitudes at $q \approx 1.48$ Å^{-1} is related to correlations involving alkyl chains carbon atoms, as their number increases with the chain length.

As for [bmim], the cation–anion contribution is found strongly negative also for [hmim] and [omim] at 0.95 Å^{-1} with minor differences for the three materials [Fig. 5(c)]. Also

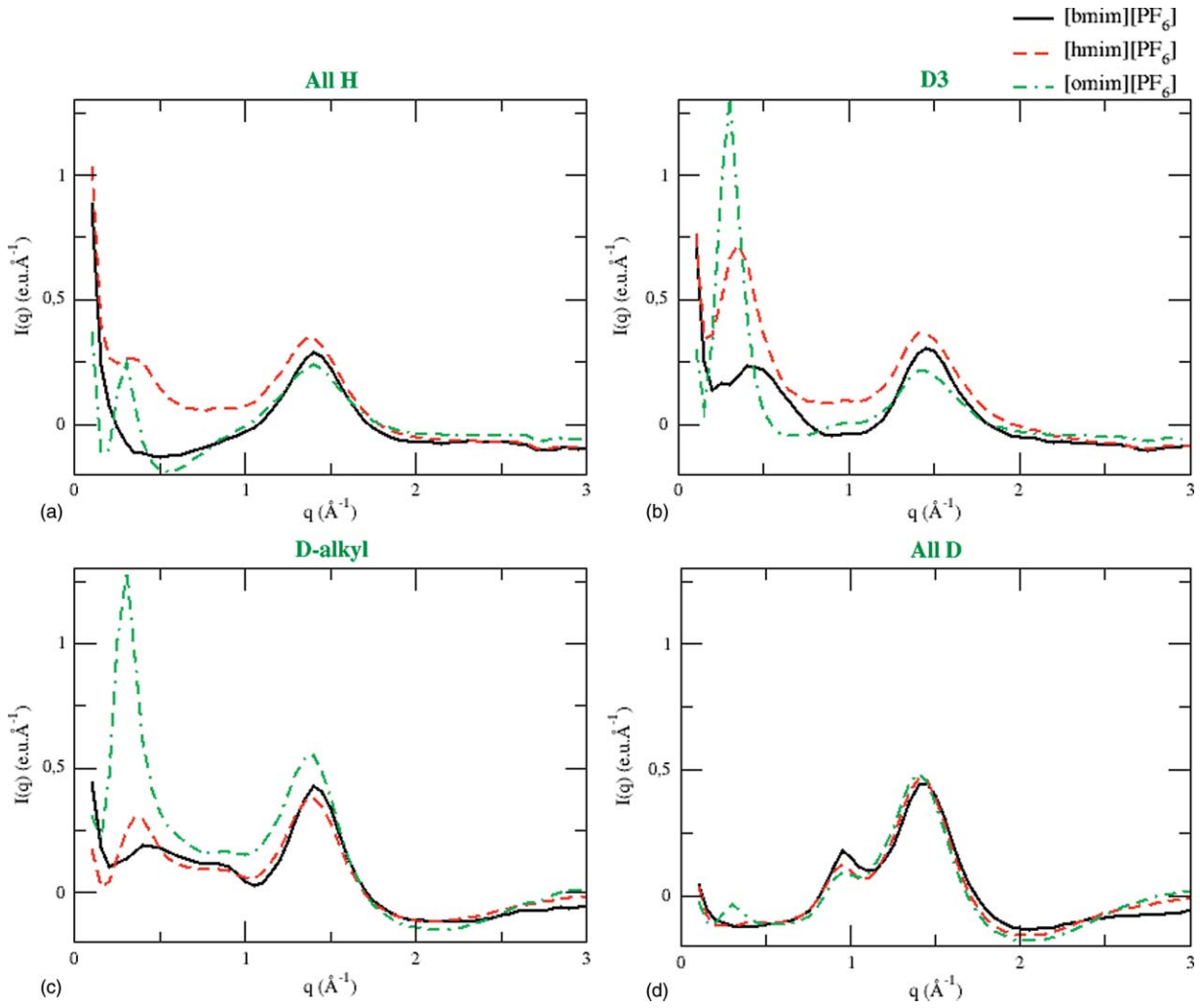

FIG. 9. Experimental neutron structure functions of [bmim][PF_6], [hmim][PF_6], and [omim][PF_6] (a), and their methyldeuteriated (b), alkyldeuteriated (c), and fully deuteriated (d) samples.

for anion–anion [Fig. 5(d)] intermolecular functions are only marginally affected by the alkyl chain length.

The structure functions obtained from MD were then compared with neutron diffraction measurements for the three molecular systems in Figs. 6(a)–8(a).[48] Panels (b)–(d) of Figs. 6–8 show also the corresponding comparison between MD-computed and neutron diffraction measurements for the deuteriated forms of the liquids. The latter are hereinafter indicated as D3 for the methyl deuteriated forms, D9/D13/D17 for the butyl/hexyl/octyl deuteriated ones and D15/D19/D23 for three fully deuteriated samples, respectively. The agreement is good in most cases and it is an important validation for the proposed force field, considering that it had been optimized against the x-ray diffraction data (and not for the neutron ones).

For a more accurate assignment of the neutron diffraction spectra, it is instructive to look at the changes of the structure functions measured upon progressive deuteration. Isotopic substitution leads to variations which are similar for the three species. At high q values (intramolecular region)

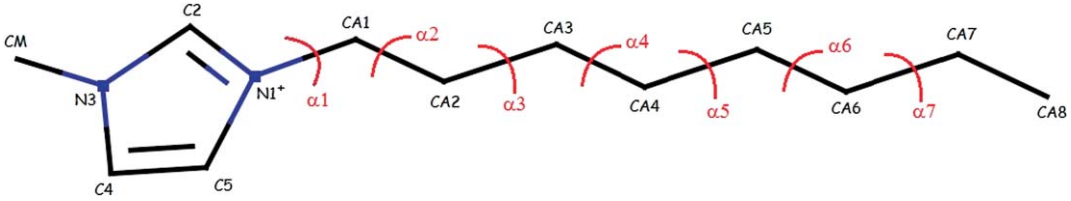

FIG. 10. Atom numbering scheme of 1-octyl-3-methylimidazolium cation.

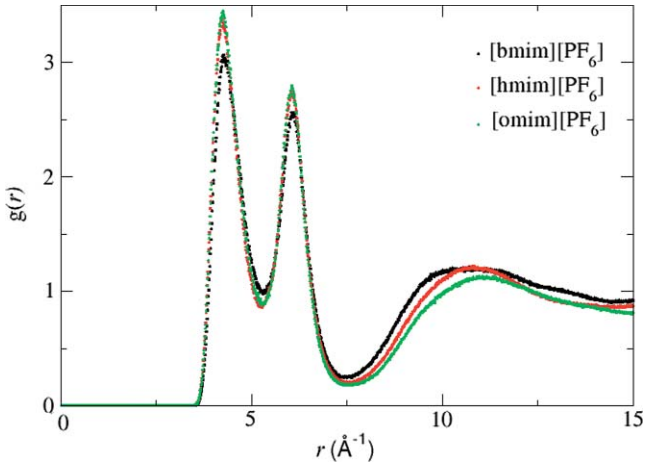

FIG. 11. $g_{P\text{-}C2}(r)$ pair correlation function. [bmim][PF_6] (black dash line); [hmim][PF_6] (red line); [omim][PF_6] (green line).

(Figs. 6–8), the experimental curves show minor changes upon methyl deuteration and more pronounced ones upon alkyl chain deuteration. However, since the region of interest to evaluate the intermolecular interactions is that at small q values, here we discuss the isotopic effects in this range and Fig. 9 reports the curves for all the three systems. We focus the attention on the three peaks (0.3–0.5, 0.95, and 1.48 $Å^{-1}$). Whatever the chain length and the degree of deuteration, the peak at 1.48 $Å^{-1}$ is always present. On the other hand, the peak at 0.9 $Å^{-1}$ appears in the spectra only upon fully deuteration and Fig. 9(d) suggests that its amplitude decreases as the alkyl chain gets longer.

To better identify its origin, partial structure functions were inspected for fully deuteriated [bmim][PF_6] by isolating the contribution of seven units: PF_6, imidazolium ring, methyl group, the three CH_2 terms of the butyl chain, and the last CH_3 of the chain. Partial structure functions were obtained by selecting each unit and considering some of their combinations to identify which pair leads to a contribution in that q range (data not shown). By such an analysis we arrive to the conclusion that the peak appearing at 0.9 $Å^{-1}$ is the fingerprint of structural correlations of the anion with the alkylic units

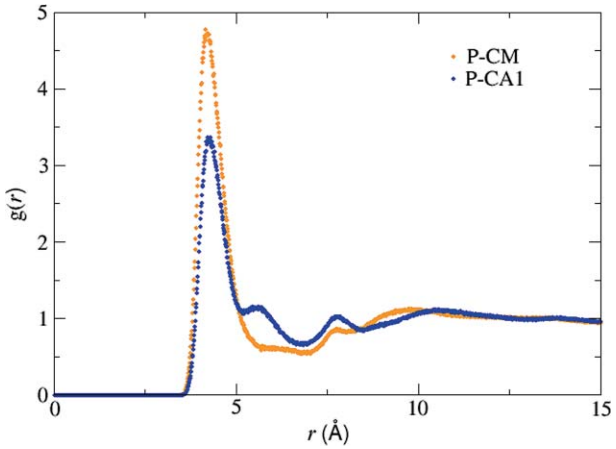

FIG. 12. P-C pair correlation function: $g_{P\text{-}CM}(r)$, (methyl) (blue line); $g_{P\text{-}CA1}(r)$, (alkyl) (orange line).

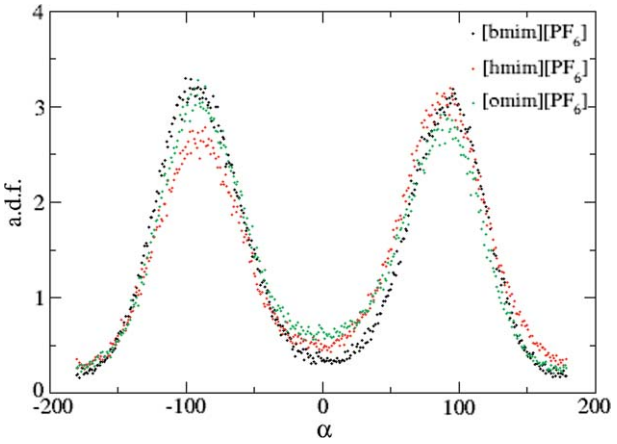

FIG. 13. Angular distribution function relative to $\alpha 1$, the dihedral angle C2–N1–CA1–CA2 for the three systems.

as well as the imidazolium ring with all the other cationic units. In conclusion, the important contributions to this region give rise to correlations between PF_6 and the cations and between cations and cations through ring and methyl groups or ring and alkyl groups. The alkyl–alkyl van der Waals interactions seem therefore to play a minor role in agreement with the analysis made by Hardacre *et al.* on the basis of the experimental differential cross section for different isotopomers.[48]

On the contrary the low q peak is strongly affected by the chain length and, as observed in the x-ray spectra, it is more intense in the system with the longest chain.[31] Selective deuteration of either of the two alkyl groups produces changes in its amplitude. When deuteration is full, the peak is quite weak in all the compounds [Fig. 9(d)].

B. Anion–cation distribution

In order to add further structural details, we provided a systematic analysis of selected partial radial distribution functions (RDFs), $g(r)$. The various atomic groups of the cation are indicated as shown in Fig. 10. The cation–anion distribution was analyzed using the P-C2 RDF, $g_{P\text{-}C2}(r)$ (Fig. 11). This function exhibits two peaks for the three systems at $r \approx 4.25$ Å and at $r \approx 6.05$ Å and a broad and weaker peak at higher values (about 11 Å). Interestingly, our simulations predict the first peak less intense than that obtained by previous MD studies[73,74] but in agreement with the results of *ab initio* simulations.[81] The two peaks' positions are very close to those of the P-C2 distances found in the crystal of [mmim][PF_6].[42] The crystal structure shows in fact two ionic pairs related through a center of symmetry at P-C2 distances equal to 3.79 and 6.17 Å.[42] The distribution of anions around the cation seems therefore show important similarities between liquid and crystal in agreement with the features of other systems such as ethyl-methylimidazolium bromide.[59]

Integration of $g_{P\text{-}C2}(r)$ up to the first minimum (5.2 Å) yields a number of coordinations close to two for all the species (2.1 for [bmim], 1.9 for [hmim], and 1.8 for [omim]) whereas integration up to the second minimum (7.5 Å) gives values which decrease with the size of the alkyl chain (5.8 for

TABLE II. Integrals for [bmim][PF_6], [hmim][PF_6], and [omim][PF_6] for $g_{P\text{-}CM}(r)$, and $g_{P\text{-}CA1}(r)$.

	$g_{P\text{-}CM}(r)$			$g_{P\text{-}CA1}(r)$		
Integration radius	$r = 5.5$ Å	$r = 7.0$ Å	$r = 10$ Å	$r = 5.5$ Å	$r = 7.0$ Å	$r = 10$ Å
[bmim][PF_6]	3.1	4.3	11.9	2.5	4.3	11.8
[hmim][PF_6]	2.9	4.0	10.4	2.4	4.4	10.1
[omim][PF_6]	2.6	3.6	9.0	2.2	3.6	8.7

[bmim], 5.3 for [hmim], and 4.8 for [omim]). This result suggests, in agreement with other reports,[48,74] that the anionic–cationic distribution is sensitive to the size of the alkyl chain. The reduction of the coordination number reflects the steric hindrance of the alkyl group which progressively increases in the series by reducing the available space around the cation.

Whereas it is known from *ab initio* calculations[16–19] that the cation site where the anion prefers to interact is C2, it is interesting to investigate whether PF_6^- shows a preferential correlation to one of the two alkyl groups. Within this aim we report in Fig. 12 the two radial distribution functions for P-CM (where CM is the carbon atom of the methyl group), $g_{P\text{-}CM}(r)$, and for P-CA1 (where CA1 is the first carbon atom of the alkyl chain), $g_{P\text{-}CA1}(r)$, for [bmim][PF_6]. The corresponding pair correlation functions (PCFs) were also obtained for [hmim][PF_6] and [omim][PF_6]. In both PCFs we observe a first sharp peak at about 4.3 Å followed by some quite low signals at about 5.3, 7.6, and 11 Å for $g_{P\text{-}CM}(r)$, and at 7.6 and 9.5 Å for $g_{P\text{-}CA1}(r)$. The data reveal a prevailing distribution of the P atom in proximity of CM rather than CA1. The presence (in both RDFs) of peaks at high r values (7.6–11 Å) indicates the existence of quite long spatial correlations. In Table II we report the values of the integrals for $g_{P\text{-}CM}(r)$ and $g_{P\text{-}CA1}(r)$ pairs calculated up to different r values for the three systems.

If integration is made up to small distances, the values of integrals confirm that PF_6^- preferentially approaches the methyl group. However, the values of the integrals become more and more similar for the three systems when the radius of integration increases. It means that at long distances (7–10 Å) the coordination numbers anion-CM and anion-CA1 get quite similar. In addition, it emerges that the integrals decrease their values with the chain size, as already found also for $g_{P\text{-}CA1}(r)$, consistently with the increasing steric hindrance of the alky group. The preferential orientation of the anion toward the methyl group is also confirmed from the spatial distribution analysis (data not shown).

C. The conformation of the alkyl chain

The conformation of the alkyl chain was also investigated through the study of angular distribution functions (ADFs) for different dihedral angles. Fig. 13 shows the ADFs with respect to $\alpha 1$, C2–N1–CA1–CA2, the dihedral angle which defines the orientation of the initial fragment of the chain for all the molecular systems. The existence of two practically equivalent rotamers ($\alpha 1 = \pm 90^\circ$) is fully consistent with the results of previous simulations,[74] with the structures of isolated ion-couples obtained from quantum chemistry,[19] and with the crystal structure[45] where the butyl group is perpendicularly oriented (82.29°) with respect to the imidazolium ring.

We further investigated the conformation of the remaining part of the alkyl chain by analyzing progressively all the dihedral angles, starting from the first one, N1–CA1–CA2–CA3, up to the end of the chain. Fig. 14 displays all the angular distribution functions for such dihedral angles, from $\alpha 3$ to the last one, $\alpha 7$, for [omim][PF_6]. The curves indicate that the alkyl chain mostly tends to assume the all-trans conformation as there is only a minor dihedral population for the gauche conformations ($\pm 60^\circ$). The existence of gauche conformers was also revealed from previous MD

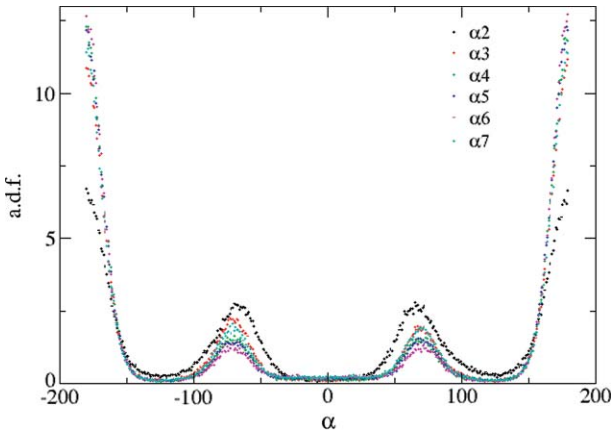

FIG. 14. Angular distribution functions relative to the conformational dihedral angles of the alkyl chain, from $\alpha 2$, N1–CA1–CA2–CA3, up to the last one $\alpha 7$, CA5–CA6–CA7–CA8, for [omim][PF_6].

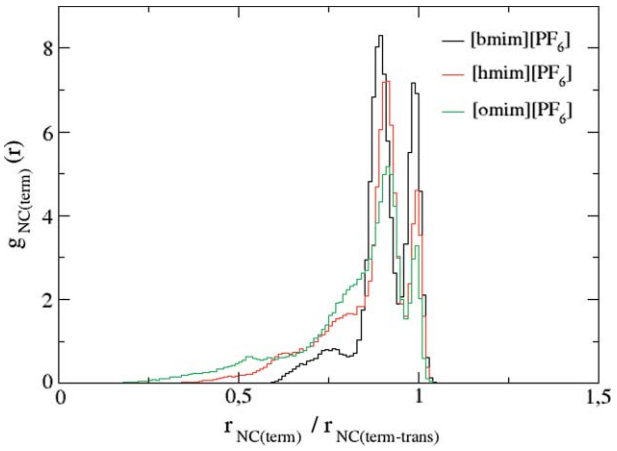

FIG. 15. Area-normalized radial distribution function $g_{NC(term)}(r)$ between nitrogen and the terminal carbon of the chain against $r_{NC(term)}/r_{NC(term\text{-}trans)}$ ($r_{NC(term\text{-}trans)}$ is the value of the $r_{NC(term)}$ when the conformation of the alkylic chain is all-trans).

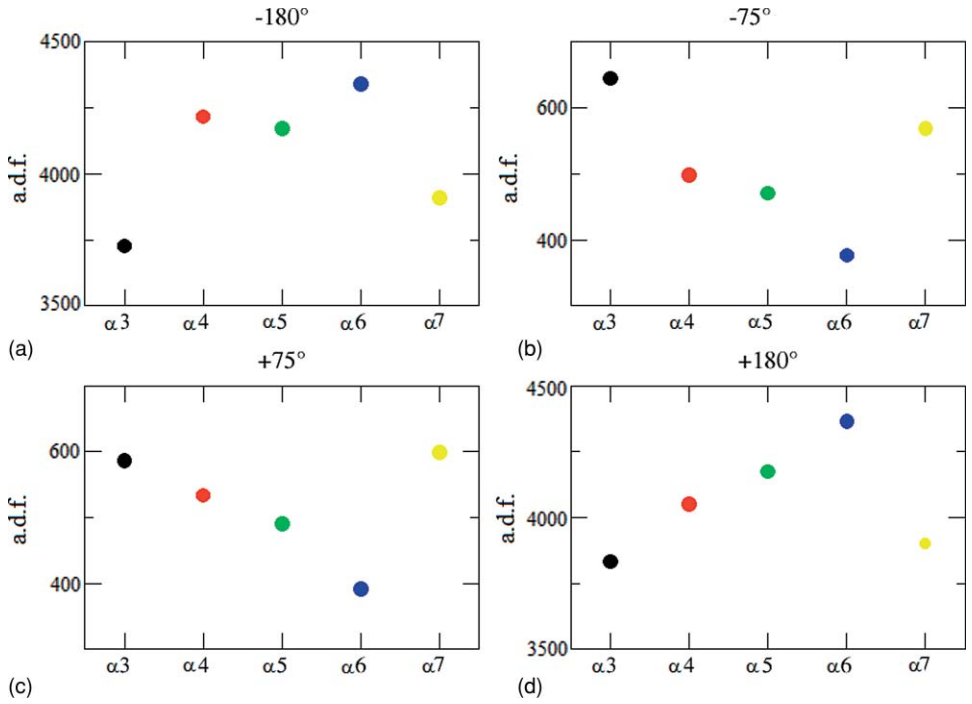

FIG. 16. Angular distribution functions relative to the conformational dihedral angles of the alkyl chain, from $\alpha 3$, CA1–CA2–CA3–CA4, up to the last one $\alpha 7$, CA5–CA6–CA7–CA8, for [omim][PF_6] when dihedral angles $= -180°$ (a), dihedral angles $= -75°$ (b), dihedral angles $= +75°$ (c), and dihedral angles $= +180°$ (d).

simulations[74] although at extent negligible. The coexistence of three conformers emerging from our simulations was found for [bmim][PF_6] in the liquid, supercooled liquid, and glass states from a recent Raman spectroscopic and calorimetric investigation.[100] As a matter of fact, quantum chemical calculations localized nine conformers for the [bmim] cation[101] and such a result is in agreement with our conformational analysis which predicts also for the third dihedral angle $\alpha 3$, a gauche-trans equilibrium, similar to the findings for the omim cation (see Fig. 14). The high number of conformers expected for [alkyl-mim][PF_6] is better displayed by Fig. 15 where the area-normalized radial distribution function between the nitrogen and the terminal carbon of the chain, $g_{NC(term)}(r)$, is reported against the ratio between the distance $r_{NC(term)}$ and the value of the same distance when the conformation is all-trans. In addition to gauche(G)/trans(T), trans(T)/trans(T) and gauche′(G′)/trans(T) conformers, Fig. 15 reveals also the existence of G/G, G′/G, G′/G′, and G/G′ conformers. The plot indicates that upon increasing the alkyl chain length the all-trans population tends to decrease in favor of more disordered conformations.

Our model further predicts that the conformer population progressively changes in favor of anti by moving toward the end of the chain. This is observed up to the $\alpha 4$ for hmim and $\alpha 6$ for omim (see Fig. 16). On the other hand, the terminal part of the chain of hmim and omim shows a sharper preference for the gauche conformer, thus suggesting a higher conformational mobility at the end of the chain.

VI. CONCLUSIONS

In this paper, energy dispersed x-ray and neutron diffraction data are presented on a series of 1-alkyl-3-methylimidazolium-hexafluorophosphates (alkyl = butyl, hexyl, and octyl). In the case of neutron diffraction data from different selectively deuteriated samples are also presented.[48]

Molecular dynamics simulations were performed employing a modified version of Lopes–Pádua force field, in order to describe both bulk properties, such as density and heats of vaporization, and x-ray diffraction data. The theoretical model, once refined on these basis, reproduces with good accuracy the neutron diffraction spectra of four isotopically substituted, fully protiated, deuteriated, 1-alkyl deuteriated, and 3-methyl deuteriated samples.

On the basis of this validated potential, further structural details were obtained from the partial radial distribution functions extracted from the MD simulations. The peaks in the cation–anion radial distribution function are consistent with an ionic distribution close to that found in the crystal of [mim][PF_6] and [bmim][PF_6] and are only slightly sensitive to the size of the alkyl chain. The data reveal in addition that the [PF_6] anion prefers to approach the methyl group rather than the alkyl chain in all the investigated systems. The angular distribution functions for different dihedral angles of the alkyl group show that the chain is perpendicularly oriented with respect to the imidazolium ring for all the molecular systems. In addition the alkyl chain is preferentially all-trans oriented along with a minor population for the gauche conformations. The all-trans population tends to decrease in favor of more disordered conformations by increasing the length of the chain. Finally a higher conformational mobility was predicted for long alkyl groups by moving toward the end of the chain.

ACKNOWLEDGMENTS

Financial support from CASPUR (Centro di Applicazione di SuperCalcolo per Università e Ricerca-Rome

Supercomputing Center)—Standard Grant 2010 std10-229, is acknowledged. Alessandro Triolo acknowledges support from the FIRB "Futuro in Ricerca" research project (RBFR086BOQ_001, "Structure and dynamics of ionic liquids and their binary mixtures").

[1] T. Welton, Chem. Rev. **99**, 2071 (1999).
[2] P. Wasserscheid and W. Keim, Angew. Chem. Int. Ed. **39**, 3772 (2000).
[3] H. Weingärtner, Angew. Chem. Int. Ed. **47**, 654 (2008).
[4] C. A. Angell, N. Byrne, and J. Belieres, Acc. Chem. Res. **40**, 1228 (2007).
[5] E. W. Castner and J. F. Wishart, J. Chem. Phys. **132**, 120901 (2010).
[6] J. F. Wishart and E. W. Castner, J. Phys. Chem. B **111**, 4639 (2007).
[7] R. D. Rogers and G. A. Voth, Acc. Chem. Res. **40**, 1077 (2007).
[8] F. Endres, Phys. Chem. Chem. Phys. **12**, 1724 (2010).
[9] *Electrochemical Aspects of Ionic Liquids*, edited by H. Ohno (Wiley-Interscience, Hoboken, 2005).
[10] P. Wasserscheid and T. Welton, *Ionic Liquids in Synthesis* (Wiley-VCH, Weinheim, Germany, 2003).
[11] V. I. Parvulescu and C. Hardacre, Chem. Rev. **107**, 2615 (2007).
[12] E. J. Maginn, J. Phys. Condens. Matter **21**, 373101 (2009).
[13] B. L. Bhargava, S. Balasubramanian, and M. L. Klein, J. Chem. Soc., Chem. Commun. **2008**, 3339.
[14] B. Kirchner, *Ionic Liquids from Theoretical Calculations in Ionic Liquids*, edited by B. Kirchner (Springer, New York, 2010), Vol. 290, p. 213.
[15] M. G. Del Pópolo, J. Kohanoff, R. M. Lynden-Bell, and C. Pinella, Acc. Chem. Res. **40**, 1156 (2007).
[16] S. B. C. Lehmann, M. Roatsch, M. Schoppke, and B. Kirchner, Phys. Chem. Chem. Phys. **12**, 7473 (2010).
[17] Z. Meng, A. Dölle, and W. R. Carper, J. Mol. Struct.: THEOCHEM **585**, 119 (2002).
[18] E. R. Talaty, S. Raja, V. J. Storhaug, A. Dölle, and C. W. Robert, J. Phys. Chem. B **108**, 13177 (2004).
[19] K. Dong, S. Zhang, D. Wang, and X. Yao, J. Phys. Chem. A **110**, 9775 (2006).
[20] J. P. Armstrong, C. Hurst, R. G. Jones, P. Licence, K. R. J. Lovelock, C. J. Satterley, and I. Villar-Garcia, Phys. Chem. Chem. Phys. **9**, 982 (2007).
[21] C. Hardacre, J. D. Holbrey, S. E. J. McMath, D. T. Bowron, and A. K. Soper, J. Chem. Phys. **118**, 273 (2003).
[22] K. Matsumoto and R. Hagiwara, J. Fluorine Chem. **128**, 317 (2007).
[23] B. L. Bhargava and S. Balasubramanian, Chem. Phys. Lett. **417**, 486 (2006).
[24] V. Kempter and B. Kirchner, J. Mol. Struct. **972**, 22 (2010).
[25] S. Tsuzuki, H. Tokuda, K. Hayamizu, and M. Watanabe, J. Phys. Chem. B **109**, 16474 (2005).
[26] S. Tsuzuki, H. Tokuda, and M. Mikami, Phys. Chem. Chem. Phys. **9**, 4780 (2007).
[27] L. M. N. B. F. Santos, J. N. C. Lopes, J. A. P. Coutinho, J. M. S. S. Esperanca, L. R. Gomes, I. M. Marrucho, and L. P. N. Rebelo, J. Am. Chem. Soc. **129**, 284 (2007).
[28] A. Triolo, O. Russina, H. J. Bleif, and E. Di Cola, J. Phys. Chem. B **111**, 4641 (2007).
[29] L. Gontrani, O. Russina, F. Lo Celso, R. Caminiti, G. Annat, and A. Triolo, J. Phys. Chem. B **113**, 9235 (2009).
[30] A. Triolo, O. Russino, B. Fazio, G. B. Appetecchi, M. Carewska, and S. Passerini, J. Chem. Phys. **130**, 164521 (2009).
[31] D. Xiao, L. G. Hines, S. Li, R. A. Bartsch, E. L. Quitevis, O. Russina, and A. Triolo, J. Phys. Chem. B **113**, 6426 (2009).
[32] O. Russina, A. Triolo, L. Gontrani, R. Caminiti, D. Xiao, L. G. Hines, R. A. Bartsch, E. L. Quitevis, N. Pleckhova, and K. R. Seddon, J. Phys. Condens. Matter **21**, 424121 (2009).
[33] O. Russina, M. Beiner, C. Pappas, M. Russina, V. Arrighi, T. Unruh, C. L. Mullan, C. Hardacre, and A. Triolo, J. Phys. Chem. B **113**, 8469 (2009).
[34] A. Triolo, O. Russina, B. Fazio, R. Triolo, and E. Di Cola, Chem. Phys. Lett. **457**, 362 (2008).
[35] J. D. Holbrey and K. R. Seddon, J. Chem. Soc., Dalton Trans. 2133 (1999).
[36] C. Hanne, S. Price, and R. Lynden-Bell, Mol. Phys. **99**, 801 (2001).
[37] A. D. MacKerell, Jr. D. Bashford, M. Bellott, R. L. Dunbrack, J. D. Evanseck, M. J. Field, S. Fisher, J. Gao, H. Guo, S. Ha, S. Joseph-McCarthy, L. Kuchnir, K. Kuczera, F. T. K. Lau, C. Mattos, S. Michnick, T. Ngo, D. T. Nguyen, B. Prodhom, W. E. Reiher III, B. Roux, M. Schlenkrich, J. C. Smith, R. Stote, J. Straub, M. Watanabe, J. Wiorkiewicz-Kuczera, D. Yin, and M. Karplus, J. Phys. Chem. B **102**, 3586 (1998).
[38] W. D. Cornell, P. Cieplak, C. I. Bayly, I. R. Gould, K. M. Merz, D. M. Ferguson, D. C. Spellmeyer, T. Fox, J. W. Caldwell, and P. A. Kollman, J. Am. Chem. Soc. **117**, 5179 (1995).
[39] W. L. Jorgensen, D. S. Maxwell, and J. Tirado-Rives, J. Am. Chem. Soc. **118**, 11225 (1996).
[40] J. N. Canongia Lopes and A. A. H. Pàdua, J. Phys. Chem. B **110**, 19586 (2006).
[41] B. L. Bhargava, R. Devane, M. L. Klein, and S. Balasubramanian, Soft Matter **3**, 1395 (2007).
[42] J. D. Holbrey, W. M. Reichert, M. Nieuwenhuyzen, O. Sheppard, C. Hardacre, and R. D. Rogers, J. Chem. Soc., Chem. Commun. **2003**, 476.
[43] C. Hardacre, S. E. J. McMath, M. Nieuwenhuyzen, D. T. Bowron, and A. K. Soper, J. Phys: Condens. Matter **15**, S159 (2003).
[44] A. R. Choudhury, N. Winterton, A. Steiner, A. I. Cooper, and K. A. Johnson, J. Am. Chem. Soc. **127**, 16792 (2005).
[45] S. M. Dibrov and J. K. Kochi, Acta Crystallogr., Sect. C: Cryst. Struct. Commun. **62**, o19 (2006).
[46] M. Kanakubo, T. Umecky, Y. Hiejima, T. Aizawa, H. Nanjo, and Y. Kameda, J. Phys. Chem. B **109**, 13847 (2005).
[47] M. Kanakubo, T. Ikeda, T. Aizawa, H. Nanjo, Y. Kameda, Y. Amo, and T. Usuki, Anal. Sci. **24**, 1373 (2008).
[48] C. Hardacre, J. D. Holbrey, C. L. Mullan, T. G. A. Youngs, and D. T. Bowron, J. Chem. Phys. **133**, 74510 (2010).
[49] L. Gontrani, F. Ramondo, and R. Caminiti, Chem. Phys. Lett. **417**, 200 (2005).
[50] L. Gontrani, F. Ramondo, G. Caracciolo, and R. Caminiti, J. Mol. Liq. **139**, 23 (2008).
[51] L. Gontrani, O. Russina, F. Lo Celso, A. Triolo, G. Annat, and R. Caminiti, J. Phys. Chem. B **113**, 9235 (2009).
[52] L. Gontrani, O. Russina, F. Cesare Marincola, and R. Caminiti, J. Chem. Phys. **131**, 244503 (2009).
[53] E. Bodo, L. Gontrani, A. Triolo, and R. Caminiti, J. Phys. Chem. Lett. **1**, 1095 (2010).
[54] R. Caminiti, M. Carbone, S. Panero, and C. Sadun, Phys. Chem. B **103**, 10348 (1999).
[55] R. Caminiti, M. Carbone, and C. Sadun, J. Mol. Liq. **75**, 149 (1998).
[56] M. Carbone, R. Caminiti, and C. Sadun, J. Mater. Chem. **6**, 1709 (1996).
[57] O. Borodin, W. Gorecki, G. D. Smith, and M. Armand, J. Phys. Chem. B **114**, 6786 (2010).
[58] K. Fujii, T. Mitsugi, T. Takamuku, T. Yamaguchi, Y. Umebayashi, and S. Ishiguro, Chem. Lett. **38**, 340 (2009).
[59] B. Aoun, A. Golbach, S. Kohara, J. F. Wax, M. A. Gonzales, and M. L. Saboungi, J. Phys. Chem. B **114**, 12623 (2010).
[60] S. Fukuda, M. Takeuchi, K. Fujii, R. Kanaki, T. Takamuku, H. Yamamoto, Y. Umebayashi, and S. Ishiguro, J. Mol. Liq. **143**, 2 (2008).
[61] R. Kanzaki, T. Mitsugi, S. Fukuda, K. Fujii, M. Takeuchi, Y. Soejima, T. Takamuku, T. Yamaguchi, Y. Umebayashi, and S. Ishiguro, J. Mol. Liq. **147**, 77 (2009).
[62] K. Fujii, Y. Soejima, Y. Kyoshoin, S. Fukuda, R. Kanzaki, Y. Umebayashi, T. Yamaguchi, S. Ishiguro, and T. Takamuku, J. Phys. Chem. B **112**, 4329 (2008).
[63] Y. Umebayashi, H. Hamano, S. Tsuzuki, J. N. C. Lopes, A. A. H. Pádua, Y. Kameda, S. Kohara, T. Yamagushi, K. Fujii, and S. Ishiguro, J. Phys. Chem. B **114**, 11715 (2010).
[64] R. W. Berg, *Ionic Liquids in Chemical Analysis: Raman Spectroscopy, Ab Initio Model Calculations and Conformational Equilibria in Ionic Liquids*, edited by M. Koel (CRC, Boca Raton, FL, 2009).
[65] R. W. Berg, Monatsch. Chem. **138**, 1045 (2007).
[66] C. Hardacre, J. D. Holbrey, and S. E. J. McMath, J. Chem. Soc., Chem. Commun. **2001**, 367.
[67] A. K. Soper, W. S. Howells, and A. C. Hannon, *ATLAS—Analysis of Time-of-Flight Diffraction Data from Liquid and Amorphous Samples*, Rutherford Appleton Laboratory, Report RAL-89-046, 1989.
[68] A. C. Hannon, W. S. Howells, and A. K. Soper, Inst. Phys. Conf. Ser. **107**, 193 (1990).
[69] A. K. Soper, Mol. Phys. **107**, 1667 (2009).
[70] T. V. Sambasivarao and O. J. Acevedo, Chem. Theory Comput. **5**, 1038 (2009).
[71] W. Smith and T. R. Forester, J. Mol. Graphics **14**, 136 (1996).

[72]See http://www.cse.clrc.ac.uk/msi/software/DLPOLY, Program version 2.17.
[73]C. J. Margulis, H. A. Stern, and J. Berne, J. Phys. Chem. B **106**, 12017 (2002).
[74]C. J. Margulis, Mol. Phys. **102**, 829 (2004).
[75]T. I. Morrow and E. J. Maggin, J. Phys. Chem. B **106**, 12807 (2002).
[76]Z. Liu, S. Huang, and W. Wang, J. Phys. Chem. B **108**, 12978 (2004).
[77]B. L. Bhargava and S. Balasubramanian, J. Chem. Phys. **127**, 114510 (2007).
[78]G. Raabe and J. K öhler, J. Chem. Phys. **128**, 154509 (2008).
[79]S. M. Urahata and M. C. C. Ribeiro, J. Chem. Phys. **122**, 24511 (2005).
[80]J. K. Shah, J. F. Brennecke, and E. J. Maginn, Green Chem. **4**, 112 (2002).
[81]B. L. Bhargava and S. Balasubramanian, Chem.Phys. Lett. **417**, 486 (2006).
[82]B. L. Bhargava and S. Balasubramanian, J. Phys. Chem. B **111**, 4477 (2007).
[83]H. V. R. Annapureddy, H. K. Kashyap, P. M. De Biase, and C. J. Margulis, J. Phys. Chem. **114**, 16838 (2010).
[84]Z. Gu and J. F. Brennecke, J. Chem. Eng. Data **47**, 339 (2002).
[85]S. V. Dzyuba and R. A. Bartsch, ChemPhysChem **3**, 161 (2002).
[86]H. Tokuda, K. Hayamizu, K. Ishii, Md. A. B. Hasan Susan, and M. Watanabe, J. Phys. Chem. B **108**, 16593 (2004).
[87]J. Jacquemin, P. Husson, A. A. H. Padua, and V. Majer, Green Chem. **8**, 172 (2006)
[88]J. G. Huddleston, A. E. Visser, W. M. Reichert, H. D. Willauer, G. A. Broker, and R. D. Rogers, Green Chem. **3**, 156 (2001).
[89]K. R. Harris and L. A. Woolf, J. Chem. Eng. Data **50**, 1777 (2005).
[90]B. Pereiro, J. L. Legido, and A. Rodriguez, J. Chem. Thermodyn. **39**, 1168 (2007).
[91]A. Muhammad, A. M. I. Mutalib, C. D. Wilfred, T. Murugesan, and A. J. Shafeeq, J. Chem. Thermodyn. **40**, 1433 (2008).
[92]T. M. Letcher and P. Reddy, J. Chem. Thermodyn. **37**, 415 (2005).
[93]A. B. Pereiro, E. Tojo, A. Rodrıguez, J. Canosa, and J. Tojo, J. Chem. Thermodyn. **38**, 651 (2006).
[94]T. M. Letcher and P. Reddy, Fluid Phase Equilib. **219**, 107 (2004).
[95]J. J. Wang, Y. Tian, Y. Zhao, and K. Zhuo, Green Chem. **5**, 618 (2003).
[96]K. R. Seddon, A. Stark, and M. J. Torres, Pure Appl. Chem. **72**, 2275 (2000).
[97]D. H. Zaitsau, G. J. Kabo, A. A. Strechan, Y. U. Paulechka, A. Tschersich, S. P. Verevkin, and A. Heintz, J. Phys. Chem. A **110**, 7303 (2006).
[98]K. Swiderski, A. McLean, C. M. Gordon, and D. H. Vaughan, J. Chem. Soc., Chem. Commun. **2004**, 2178.
[99]J. P. Armstrong, C. Hurst, R. G. Jones, P. Licence, K. R. J. Lovelock, C. J. Satterley, and I. J. Villar-Garcia, Phys. Chem. Chem. Phys. **9**, 982 (2007).
[100]T. Endo, T. Kato, K. Tozaki, and K. Nishikawa, J. Phys. Chem. B **114**, 407 (2010).
[101]S. Tsuzuki, A. A. Arai, and K. Nishikawa, J. Phys. Chem. B **112**, 7739 (2008).